A Mathematical Model of the Bulk Copolymerization of Styrene and Acrylonitrile in the Presence of Polystyrene-*block*-Polybutadiene

Daniel Elizarrarás, Graciela Morales,* Ramón Díaz de León, Carla Luciani, Diana Estenoz

The bulk copolymerization of styrene and acrylonitrile in the presence of SB using BPO as initiator was investigated. Reactions were carried out at 80 °C with different initial SB concentrations. Global variables, such as conversion and cumulative grafting efficiency of SAN, were determined during the prepolymerization. The isolated non-grafted SAN was also analyzed to determine its average molar masses and composition. A mathematical model was developed, and theoretical predictions were compared with experimental data. A good agreement between measurements and simulations was obtained from a heterogeneous model when BPO was evenly distributed between phases.

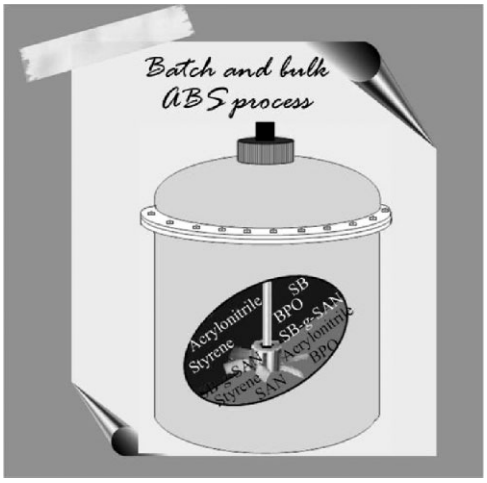

Introduction

The acrylonitrile-butadiene-styrene (ABS) polymer is a heterogeneous material of great commercial importance. It is composed of a continuous poly(styrene-*co*-acrylonitrile) (SAN) matrix containing a dispersion of rubber particles. The final material exhibits high impact strength with little compromise of its modulus respective to SAN. Processing properties are determined not only by the molecular weight distribution (MWD) of the non-grafted SAN matrix but also by the rubber particles characteristics.[1,2] In turn, these properties are determined during its synthesis, which can be either by successive steps of emulsion polymerization or by bulk (or bulk/suspension) copolymerization of styrene (S) and acrylonitrile (AN) in the presence of a rubber. The former process usually yields rubber particles with core/shell morphologies, where the core is of rubber and the shell is of a graft terpolymer produced by the radicals attack onto the rubber. The latter process also yields heterogeneous rubber particles, but, in this case, the rubber particles contain numerous SAN

D. Elizarrarás, G. Morales, R. Díaz de León
Centro de Investigación en Química Aplicada CIQA, Blvd. Enrique Reyna 140, Saltillo 25253, Coahuila, México
Fax: +52 844 438 9839; E-mail: gmorales@ciqa.mx
C. Luciani, D. Estenoz
Instituto de Desarrollo Tecnológico para la Industria Química INTEC, Güemes 3450, Santa Fe S3000GLN, Argentina

Macromol. Theory Simul. **2008**, *17*, 180–197

DOI: 10.1002/mats.200800004

occlusions (salami morphology). Moreover, the bulk process allows the production of well-reinforced polymers using lower amounts of the (expensive) rubber reagent and is friendlier to the environment.

Several analogies can be found when comparing ABS with high-impact polystyrene (HIPS). The mechanical properties of both materials are mainly determined by the size, morphology, and volume fraction of the rubber particles.[3–14] Typically, HIPS is produced by polymerizing S in the presence of polybutadiene (PB), and a styrene-butadiene graft copolymer is generated from the very beginning of the reaction. Generating graft copolymer compatibilizes the phases, stabilizes the particles, and promotes the formation of particle occlusions.[15–19] When using polystyrene-*block*-polybutadiene (SB) as precursor rubber, the initial polystyrene (PS) block is compatible with the PS matrix, acts as a surfactant, reduces the interfacial tension, and promotes the formation of smaller particles.[20,21] It has been proven that a variety of rubber particle morphologies can be produced in HIPS by employing SB instead of PB, but a rather low reinforcement is obtained.[8,20,21] Some differences appear when using SB to produce ABS. Due to the PS block no longer being thermodynamically compatible with the SAN generated along the reaction, the rubber particles are relatively bigger and the morphology is of the salami type. Therefore, a better reinforcement is generally obtained.[22,23]

Over the last 30 years, the HIPS process has been theoretically investigated through homogeneous and heterogeneous mathematical models.[24–38] The former assume polymerization taking place in a single phase. Such an assumption is strictly valid for solution polymerizations and for bulk polymerizations at very low conversions. In the bulk process at relatively low monomer conversions of 0.5–2%, phase separation occurs due to the thermodynamic incompatibility between PS and PB chains.[16,34–41] Experimental studies involving blends that emulate the bulk process have shown that low molar mass species, such as monomer, chain transfer agent, and initiators, are evenly partitioned between the phases when the system has reached thermodynamic equilibrium.[38–41] These uniform distributions have justified the use of homogeneous models at conditions where phase separation has already occurred. Heterogeneous models consider the polymerization taking place in 2 phases that instantaneously reach thermodynamic equilibrium.[36–38,41] This assumption implies a very fast transfer of reagents and products between phases with respect to the rate of polymerization.[36,37,41]

The bulk process for the production of ABS has been scarcely investigated. In a series of articles, Locatelli and Riess[42–46] studied different moderately-concentrated solution copolymerizations of S and AN in the presence of PB. They also investigated the equilibrium distributions of comonomers and benzoyl peroxide (BPO) initiator from blends that emulate the polymerization. Measurements indicated that SAN chains grafted onto PB exhibited a relatively lower AN content than the non-grafted chains.[42] The authors suggested that this was a consequence of a slightly preferential accumulation of S in the PB-rich phase.[42] The molecular weights of the grafted SAN were noticeable higher than those of the non-grafted SAN.[43] This was explained in terms of the different compositions and nature of the phases where grafted and non-grafted SAN are generated. Measurements from blends containing benzene/SAN/PB/BPO and benzene/AN/SAN/PB/BPO showed that initiator concentration was about three times higher in the PB-rich phase than the corresponding concentration in the SAN-rich phase.[44] Locatelli and Riess[45,46] modeled the copolymerization of S and AN in the presence of PB. To this purpose, a simple kinetic mechanism involving initiation, propagation, and termination was proposed, and rather empiric correlations were employed for estimating initiator efficiencies, initiator concentrations, and termination rate constants in each phase.[46] Hayes et al.[47,48] carried out kinetic studies at low conversions in dilute solution copolymerizations of S and AN in the presence of PB. When a poor promoter of grafting such as 2,2′-azoisobutyronitrile (AIBN) was used as initiator, the kinetics could be described as a copolymerization between an average (S + AN) monomer and butadiene repeating units. However, the model was not useful for describing reactions with other initiators that promote the rubber grafting. Bouquet et al.[49] measured the mass of non-grafted rubber as a function of the reaction time along several bulk copolymerizations of S and AN in the presence of PB and AIBN, bis(2-methylbenzoyl) peroxide, dibenzoyl peroxide, and 1,1-bis(*tert*-butyl peroxide) cyclohexane. They found that the mass of non-grafted SAN was related with the rate of initiator decay.

In this work, a novel mathematical model to simulate the batch and bulk copolymerization of S and AN in the presence of SB is presented. The evolution of the global variables and polymer molecular macrostructures are estimated with the final aim of qualifying the performance of the proposed model to fit experimental measurements during the prepolymerization stage.

Experimental Part

Materials

Base materials involve S and AN comonomers, BPO initiator, and a SB rubber. Industrial grades of S and SB were kindly supplied by Dynasol Elastómeros (México). Rubber exhibited a butadiene content of 60 wt.-% with 8.5 wt.-% of 1,2-vinyl units. BPO initiator was supplied by Promotores y Catalizadores Orgánicos de México.

Table 1. Recipes.

	Reaction A	Reaction B
	wt.-%	wt.-%
S	72.72	68.07
AN	21.23	19.88
SB	6.00	12.00
BPO	0.05	0.05

A reagent grade AN was purchased from Aldrich Co. Initiator was recrystallized from a chloroform solution by addition of methanol, filtration, and drying under vaccum at room temperature until constant weight was reached. The other reagents were used as received.

Polymerization Reactions

A preliminary set of reactions was carried out. For space reasons, only 2 polymerizations are presented in this article (Table 1). In order to avoid copolymer compositional drift along the reaction, the comonomer feed ratio was chosen close to the theoretical azeotropic point of the SAN copolymerization (i.e., 23 wt.-% of AN). The initial weight content of butadiene repeating units in reaction A was of 3.6 wt.-% (6.0 wt.-% SB), while in reaction B it was of 7.2 wt.-% (12 wt.-% SB). Comonomers and rubber were fed into a 1 gallon stainless steel reactor equipped with an anchor and a turbine stirrer. The reaction system was purged with nitrogen, and the mixture was stirred for about 12 h at room temperature. After complete SB dissolution, BPO initiator was added, and the system was purged again. This solution was gradually heated up from room temperature to 80 °C, over a 90 min period. It is assumed that monomers did not react during the initial heating-up period due to the presence of antioxidants, thermal stabilizers, and inhibitors contained in the S, AN, and SB. Thereafter, temperature was kept constant at 80 °C (with a maximum deviation of 1.5 °C) and the reaction mixture was stirred at 70 rpm. Reactions were carried out up to comonomers conversion close to 45%. (Higher conversions were not analyzed because preliminary studies showed that only the prepolymerization stage is important for the development of the rubber particle morphology).[22,23]

Sample Characterization

Samples taken from the reactor at increasing conversions were promptly cooled with ice. In each sample, a small portion was first weighted (m_s) and then dissolved in a (50:50 v/v) toluene/methyl ethyl ketone solution containing hydroquinone as inhibitor. The polymer was precipitated with an excess of methanol, filtered, and dried under vacuum at 40 °C until constant weight (m_p) was reached. The comonomer conversion (x), defined as the ratio between the mass of polymerized comonomers (i.e., grafted and non-grafted SAN) and the initial mass of comonomers, was calculated through Equation (1):

$$x = \frac{m_p - m_s w_{SB}^0}{m_s(1 - w_{SB}^0)} \quad (1)$$

where w_{SB}^0 is the weight fraction of SB in the reaction recipe.

The non-grafted SAN was separated from the polymer mixture (i.e., non-grafted SAN + unreacted SB + SB-*g*-SAN) through a solvent extraction technique that employed acetone as selective solvent for the non-grafted SAN.[50] The extraction involved 5 consecutive cycles of a 24 h under agitation followed by ultracentrifugation at 20 °C and 21 000 rpm. The soluble fraction was first isolated with the help of a syringe, and then concentrated by rotoevaporation, precipitated with methanol, and dried until

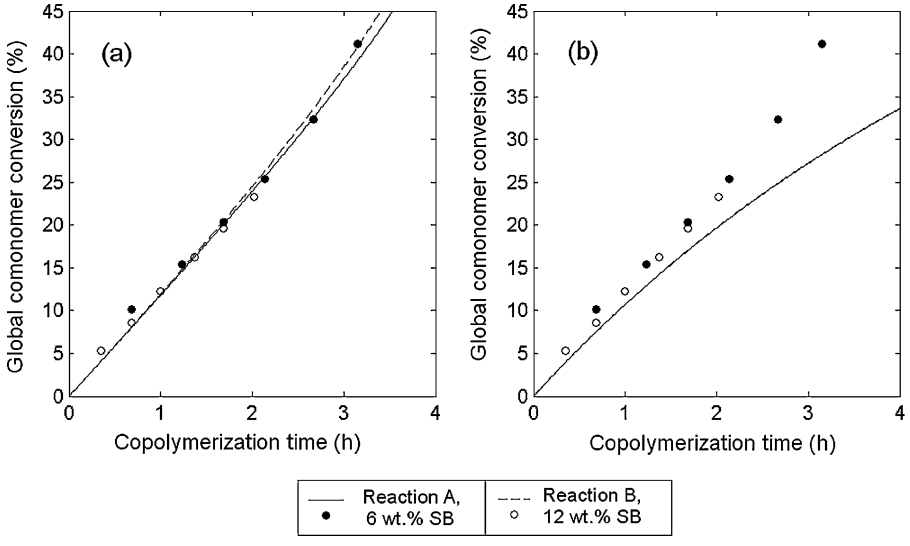

Figure 1. Evolution of comonomer conversion. Experimental data are represented by symbols and simulation results of the Heterogeneous Model with $K_l = 1$ are represented by traces. a) Theoretical results taking into account the gel effect; and, b) Theoretical results neglecting the gel effect.

Macromol. Theory Simul. **2008**, *17*, 180–197

Macromolecular Journals

DOI: 10.1002/mats.200800004

constant weight at room temperature (m_{ngSAN}). The absence of SB in the non-grafted SAN was confirmed by 300 MHz resolution ^{1}H NMR. The cumulative SAN grafting efficiency (E_{SAN}), defined as the ratio between the mass of grafted SAN and the mass of polymerized comonomers, was calculated through Equation (2):

$$E_{SAN} = \frac{m_p - m_{ngSAN} - m_s w^0_{SB}}{m_p - m_s w^0_{SB}} = \frac{m_p - m_{ngSAN} - m_s w^0_{SB}}{x\, m_s (1 - w^0_{SB})} \quad (2)$$

Based on the results of the preliminary set of reactions, the experimental errors related to the measurement of conversion and cumulative grafting efficiency are about 1.76 and 0.94%, respectively. These error bands will be considered later for the model adjustment.

The molecular weight distribution (MWD) of the non-grafted SAN was measured by size exclusion chromatography (SEC). To such effect, a Hewlett Packard HPLC 1100 chromatograph was fitted with a set of three columns with nominal pore diameters of 10^3, 10^5 and 10^6 Å. The solvent was tetrahydrofuran at 1 mL · min^{-1}. The MWD and its average values were first referred to PS standards, and then corrected by the universal calibration method.[51] The fraction containing the unreacted SB + SB-*g*-SAN was also analyzed by SEC. Finally, the average AN content in the non-grafted SAN ($\overline{w}_{AN,ngSAN}$) was determined by ^{1}H NMR, relating the areas under the aliphatic (1–3 ppm) and aromatic (6.2–7.5 ppm) protons.

Measurements of conversion, cumulative SAN grafting efficiency, and average molecular weights and composition of the non-grafted SAN are represented by symbols in Figure 1–4, and the following is observed: a) conversion increases almost linearly with the reaction time, and it seems to be unaffected by the initial rubber concentration (Figure 1); b) the cumulative SAN grafting efficiency drops along the reactions, and higher grafting efficiencies are obtained for reaction B due to its also higher initial rubber concentration (Figure 2); c) the average molecular

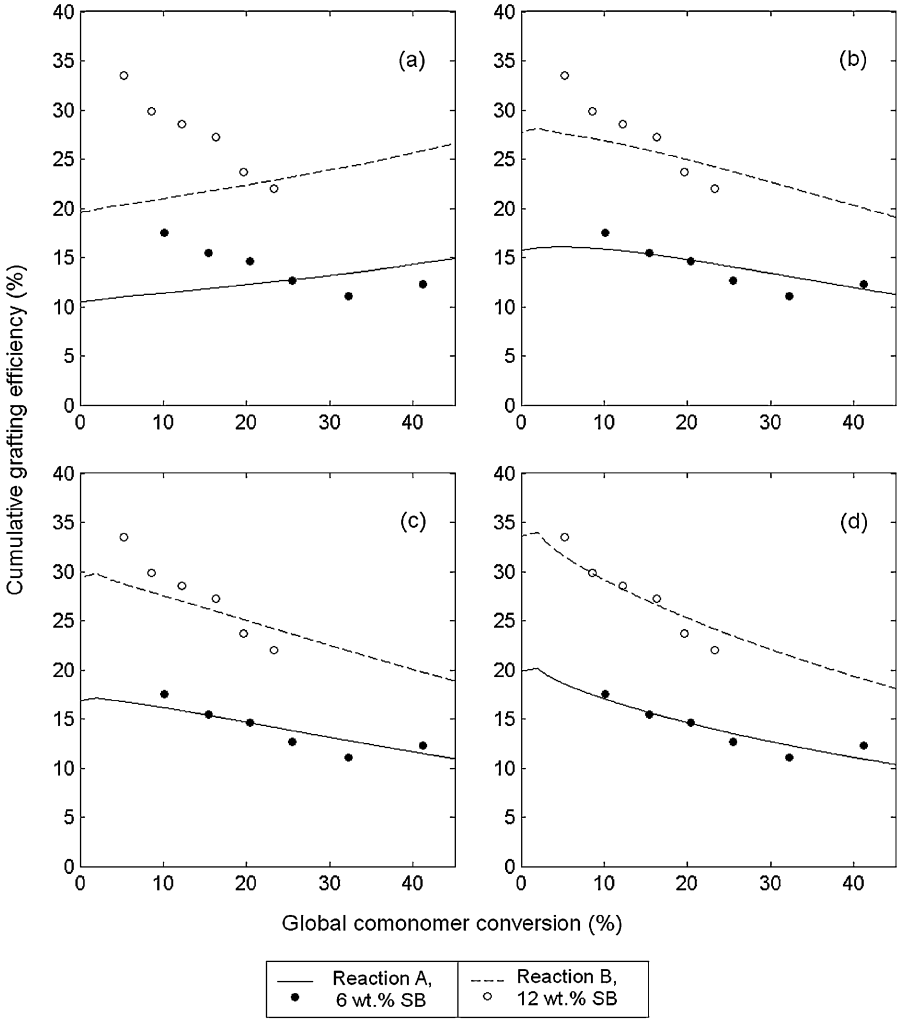

Figure 2. Evolution of the cumulative SAN grafting efficiency. Experimental data are represented by symbols and simulation results are represented by traces. a) Homogeneous model; b) Heterogeneous model with $K_I = 3$; c) Heterogeneous model with $K_I = 2$; and, d) Heterogeneous model with $K_I = 1$.

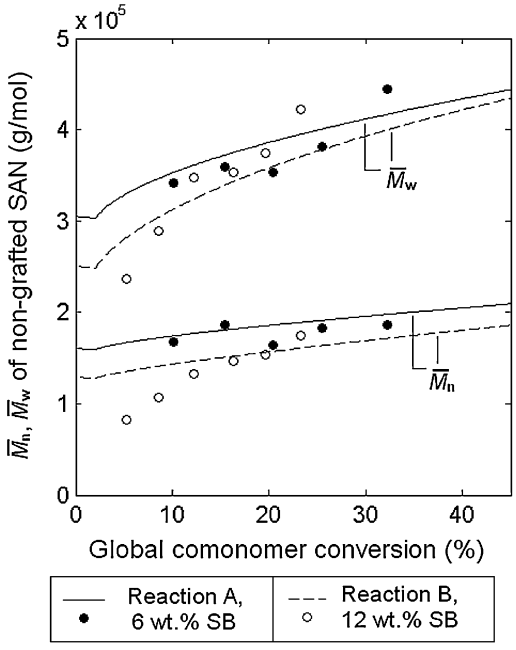

Figure 3. Average molecular weights of non-grafted SAN. Experimental data are represented by symbols and simulation results of the heterogeneous model with $K_I = 1$ are represented by traces.

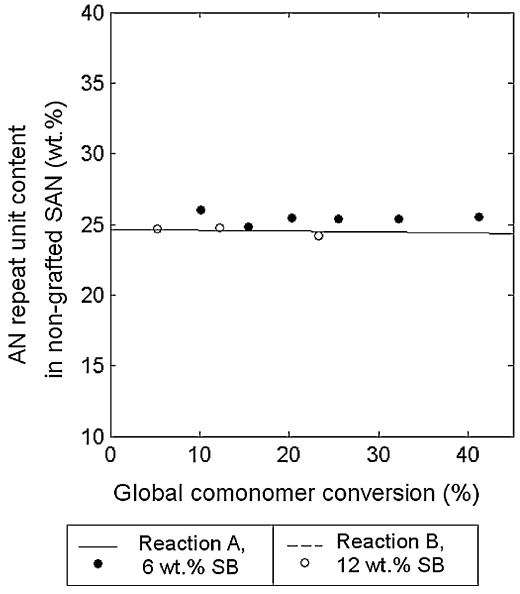

Figure 4. Average AN content in the non-grafted SAN. Experimental data are represented by symbols and simulated results of the heterogeneous model with $K_I = 1$ are represented by traces.

weights of the non-grafted SAN increase along the reaction, and the values are quite overlapped for reactions A and B (Figure 3); and, d) the average composition of the non-grafted SAN is essentially constant as the conversion increases, and it is almost unaffected by the rubber initial concentration (Figure 4). The reasons for all these trends will be discussed later, together with the simulation results.

Figure 5 shows the chromatograms of the isolated non-grated SAN and unreacted SB + SB-*g*-SAN fractions at $x = 8.6$ and 23.3%, corresponding to reaction B. Each chromatogram was normalized separately. It is observed that non-grafted SAN chromatograms are wider and monomodal, while unreacted SB + SB-*g*-SAN chromatograms are bimodal. The increasing shoulders in the left hand side of the unreacted SB + SB-*g*-SAN chromatograms is due to the generation of the terpolymer, while the main peak basically corresponds to the unreacted (and almost monodisperse) SB. The fact that the main SB peak is retained at increasing conversions suggests that the non-grafted SAN (of relatively high polydispersity) was completely separated from the SB + SB-*g*-SAN mixture.

Mathematical Modeling

Kinetic Mechanism

The kinetic mechanism adopted for describing the copolymerization of S and AN in the presence of SB is presented in Table 2. It considers chemical initiation, thermal initiation of S, propagation, chain transfer reactions to the comonomers and to the rubber, and termination by recombination of macroradicals. Termination by disproportionation and pure crosslinking of SB due to combination of butadienyl radicals are neglected.[35,52–58] Comonomers, initiator, and unreacted butadiene repeating units in SB are indicated as S, AN, I, and B, respectively. The primary radicals of S, AN, I, and B are represented by $S_1^\bullet$, $AN_1^\bullet$, $I^\bullet$, and $B^\bullet$, respectively. Primary radicals of a terpolymer molecule produced by addition of a monomer unit onto $B^\bullet$ are indicated as $TS_1^\bullet$ and $TAN_1^\bullet$, respectively. Non-primary copolymer radicals are denoted by $S_n^\bullet$ and $AN_n^\bullet$, and non-primary terpolymer radicals are indicated by $TS_n^\bullet$ and $TAN_n^\bullet$. Note that primary and non-primary radicals are classified according to their radical end group. Dead polymers are distinguished as follows: i) non-grafted SAN copolymer molecules (C_n); ii) T-shaped SAN branches linked to a single B repeating unit (T_n); and, iii) H-shaped SAN branches linked to two B repeating units (H_n). In all cases, the subscript n is the number of repeating units in dead polymers or macroradicals. The kinetic mechanism considers that S repeating units in the original SB are non-reactive, while B units are only reactive for initiation and transfer reactions. Even though the global mechanism in Table 2 can be extended to calculate the detailed graft terpolymer topologies,[33,34] the distinction of T- and H-shaped SAN branches is enough to the purpose of this study.

With respect to the reactions in Table 2, the following assumptions are adopted: a) Reaction (R1–R41) are elementary; b) the comonomers are mainly consumed by propagation reactions; c) propagation, transfer, and termination rate constants are independent of the macroradical length; d) the gel effect is taken into account by reducing the termination rate constants of Reaction

Macromol. Theory Simul. **2008**, *17*, 180–197

Macromolecular Journals
DOI: 10.1002/mats.200800004

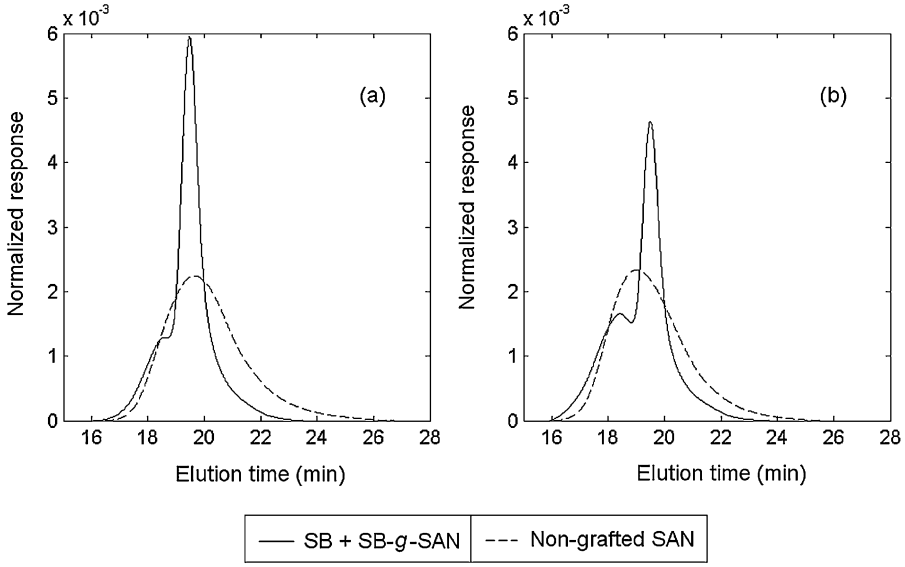

Figure 5. Size exclusion chromatograms of non-grafted SAN and unreacted SB + SB-*g*-SAN fractions of samples taken along reaction B: a) $x = 8.6\%$, b) $x = 23.3\%$.

(R28–R41) with the free volume of the system;[53,54] and, e) the reactivity of a macroradical depends on the ultimate repeating unit (i.e., terminal model). This last assumption determines that Reaction (R8–R11), (R16–R19), (R24–R25), (R28–R30), and (R38–R39) have the same rate constants as Reaction (R12–R15), (R20–R23), (R26–R27), (R31–R37), and (R40–R41), respectively.

The gel effect is introduced through a reduction of the termination rate constants. For bulk SAN polymerizations, Garcia-Rubio et al.[53] employed a correlation that depended on the copolymer weight-average molar mass and of the free volume of the system. Cavalcanti and Pinto[54] used a modified version of such correlation but independent of the SAN weight-average molar masses. In this work, this last approach is used to correct the termination rate constants, as indicated in Equation (3):[54]

$$k_{tik,j} = k^0_{tik} \exp\{-A(1/V_{f,j} - 1/V^{Cr}_{f,j})\} \quad j = 1,2; \quad i,k = a,s,b \tag{3}$$

where $k_{tik,j}$ is any of the termination rate constants in Reaction (R28–R41) corrected for the gel effect in the phase j (with $j = 1$ for the SB-rich phase and $j = 2$ for the SAN-rich phase); k^0_{tik} is the corresponding termination rate constant in absence of gel effect; A is a constant parameter that relates the gel effect to a reduction of the free volume along reaction; $V_{f,j}$ is the free volume of phase j, and $V^{Cr}_{f,j}$ is the critical free volume of phase j. Finally, $V^{Cr}_{f,1}$ and $V^{Cr}_{f,2}$ were adopted as the free volumes of the initial SB/comonomers solution and of the S and AN initial solution, respectively. Equation (4)–(6) allow the calculation of the mentioned free volumes:[53,54]

$$V_{f,j} = \sum_{i=SAN,PB,PS,S,AN} \{0.025 + \alpha_i(T - T_{g,i})\}\phi_{i,j} \quad j = 1,2 \tag{4}$$

$$V^{Cr}_{f,1} = \sum_{i=PB,PS,S,AN} \{0.025 + \alpha_i(T - T_{g,i})\}\phi^0_{i,1} \tag{5}$$

$$V^{Cr}_{f,2} = \sum_{i=S,AN} \{0.025 + \alpha_i(T - T_{g,i})\}\phi^0_{i,2}/(\phi^0_{S,2} + \phi^0_{AN,2}) \tag{6}$$

where α_i is the difference in the thermal expansion coefficient of species i above and below the glass transition temperature ($T_{g,i}$), with i = SAN, PB, PS, S, and AN (PB and PS indicates the homopolymeric blocks in the initial SB, and SAN indicates all the grafted and non-grafted copolymer); and $\phi_{i,j}$ is the volume fraction of species i in phase j, where a superscript 0 indicates the corresponding value in the initial condition.

Polymerization Model

The heterogeneous model for describing the batch and bulk copolymerization of S and AN in the presence of SB involves an initial homogeneous stage followed by a heterogeneous stage after the phase separation point. During the heterogeneous stage, the model assumes an instantaneous thermodynamic equilibrium for S, AN, and

Table 2. Global kinetic mechanism ($n, m = 0, 1, \ldots, \infty$).

Initiation

$$I \xrightarrow{k_d} 2I^{\bullet} \quad (R1)$$

$$3S \xrightarrow{k_{i0}} 2S_1^{\bullet} \quad (R2)$$

$$I^{\bullet} + S \xrightarrow{k_{is}} S_1^{\bullet} \quad (R3)$$

$$I^{\bullet} + AN \xrightarrow{k_{ia}} AN_1^{\bullet} \quad (R4)$$

$$I^{\bullet} + B \xrightarrow{k_{ib}} B^{\bullet} \quad (R5)$$

$$B^{\bullet} + S \xrightarrow{k_{bs}} TS_1^{\bullet} \quad (R6)$$

$$B^{\bullet} + AN \xrightarrow{k_{ba}} TAN_1^{\bullet} \quad (R7)$$

Propagation

$$S_n^{\bullet} + S \xrightarrow{k_{pss}} S_{n+1}^{\bullet} \quad (R8)$$

$$S_n^{\bullet} + AN \xrightarrow{k_{psa}} AN_{n+1}^{\bullet} \quad (R9)$$

$$AN_n^{\bullet} + S \xrightarrow{k_{pas}} S_{n+1}^{\bullet} \quad (R10)$$

$$AN_n^{\bullet} + AN \xrightarrow{k_{paa}} AN_{n+1}^{\bullet} \quad (R11)$$

$$TS_n^{\bullet} + S \xrightarrow{k_{pss}} TS_{n+1}^{\bullet} \quad (R12)$$

$$TS_n^{\bullet} + AN \xrightarrow{k_{psa}} TAN_{n+1}^{\bullet} \quad (R13)$$

$$TAN_n^{\bullet} + S \xrightarrow{k_{pas}} TS_{n+1}^{\bullet} \quad (R14)$$

$$TAN_n^{\bullet} + AN \xrightarrow{k_{paa}} TAN_{n+1}^{\bullet} \quad (R15)$$

Chain transfer to monomers

$$S_n^{\bullet} + S \xrightarrow{k_{fss}} S_1^{\bullet} + C_n \quad (R16)$$

$$S_n^{\bullet} + AN \xrightarrow{k_{fsa}} AN_1^{\bullet} + C_n \quad (R17)$$

$$AN_n^{\bullet} + S \xrightarrow{k_{fas}} S_1^{\bullet} + C_n \quad (R18)$$

$$AN_n^{\bullet} + AN \xrightarrow{k_{faa}} AN_1^{\bullet} + C_n \quad (R19)$$

$$TS_n^{\bullet} + S \xrightarrow{k_{fss}} S_1^{\bullet} + T_n \quad (R20)$$

$$TS_n^{\bullet} + AN \xrightarrow{k_{fsa}} AN_1^{\bullet} + T_n \quad (R21)$$

Chain transfer to the monomers (cont.)

$$TAN_n^{\bullet} + S \xrightarrow{k_{fas}} S_1^{\bullet} + T_n \quad (R22)$$

$$TAN_n^{\bullet} + AN \xrightarrow{k_{faa}} AN_1^{\bullet} + T_n \quad (R23)$$

Chain transfer to SB

$$S_n^{\bullet} + B \xrightarrow{k_{fsb}} B^{\bullet} + C_n \quad (R24)$$

$$AN_n^{\bullet} + B \xrightarrow{k_{fab}} B^{\bullet} + C_n \quad (R25)$$

$$TS_n^{\bullet} + B \xrightarrow{k_{fsb}} B^{\bullet} + T_n \quad (R26)$$

$$TAN_n^{\bullet} + B \xrightarrow{k_{fab}} B^{\bullet} + T_n \quad (R27)$$

Termination by recombination

$$S_{n-m}^{\bullet} + S_n^{\bullet} \xrightarrow{k_{tss}} C_n \quad (R28)$$

$$S_{n-m}^{\bullet} + AN_n^{\bullet} \xrightarrow{k_{tsa}} C_n \quad (R29)$$

$$AN_{n-m}^{\bullet} + AN_n^{\bullet} \xrightarrow{k_{taa}} C_n \quad (R30)$$

$$S_{n-m}^{\bullet} + TS_n^{\bullet} \xrightarrow{k_{tss}} T_n \quad (R31)$$

$$S_{n-m}^{\bullet} + TAN_n^{\bullet} \xrightarrow{k_{tsa}} T_n \quad (R32)$$

$$AN_{n-m}^{\bullet} + TS_n^{\bullet} \xrightarrow{k_{tsa}} T_n \quad (R33)$$

$$AN_{n-m}^{\bullet} + TAN_n^{\bullet} \xrightarrow{k_{taa}} T_n \quad (R34)$$

$$TS_{n-m}^{\bullet} + TS_n^{\bullet} \xrightarrow{k_{tss}} H_n \quad (R35)$$

$$TS_{n-m}^{\bullet} + TAN_n^{\bullet} \xrightarrow{k_{tsa}} H_n \quad (R36)$$

$$TAN_{n-m}^{\bullet} + TAN_n^{\bullet} \xrightarrow{k_{taa}} H_n \quad (R37)$$

$$B^{\bullet} + S_n^{\bullet} \xrightarrow{k_{tbs}} T_n \quad (R38)$$

$$B^{\bullet} + AN_n^{\bullet} \xrightarrow{k_{tba}} T_n \quad (R39)$$

$$B^{\bullet} + TS_n^{\bullet} \xrightarrow{k_{tbs}} H_n \quad (R40)$$

$$B^{\bullet} + TAN_n^{\bullet} \xrightarrow{k_{tba}} H_n \quad (R41)$$

initiator, and a complete incompatibility between SAN and SB.[36,37,42–46] Thus, all the non-grafted SAN produced in the SB-rich phase instantaneously migrates toward the SAN-rich phase.[36,37,41] Similarly, graft terpolymer instantaneously accumulates at the main interface, with its SB portion at the SB-rich phase and its SAN branches at the SAN-rich phase.[36,37,41] Because of their extremely short lifetime, macroradicals are assumed to remain in the phase where produced.[36,37,41]

The instantaneous distributions of the low molar mass species between phases are introduced through partition coefficients (K_i), defined as the ratio between the molar concentration of species i in the SB-rich phase and its concentration in the SAN-rich phase, as stated in Equation (7):

$$K_i = \frac{[i]_1}{[i]_2}; \quad (i = S, AN, I) \quad (7)$$

Macromol. Theory Simul. **2008**, *17*, 180–197

Macromolecular Journals
DOI: 10.1002/mats.200800004

where brackets indicate molar concentration, and subscripts 1 and 2 indicate the SB-rich and SAN-rich phases, respectively.

The complete heterogeneous model is presented in Appendices A and B. Appendix A involves the global balances of reagents and products, and it allows the calculation of the evolution of the species concentrations, comonomers conversion, and volumes of the phases along the reaction. The homogeneous stage before the phase separation point is solved through the balances of reagents and products in Equation (A1), (A3), (A5) and (A7)–(A13), considering a single SB-rich phase only ($j=1$). Volume contraction is calculated through Equation (A14). In the heterogeneous period after phase separation point, molar balances given by Equation (A1), (A3), (A5) and (A7)–(A13) must be solved considering the 2 coexistent phases (i.e., $j=1,\ 2$). To such effect, Equation (A2), (A4) and (A6) introduce the instantaneous distribution of the low molar mass species between the phases, and Equation (A14)–(A16) estimate the variation of the phase volumes, considering the migration of species between phases and the volume contraction. The resulting "stiff" system of differential equations is integrated by an appropriate numerical method. Finally, the global comonomers conversion is calculated through Equation (A17). In Appendix B, a pseudo-homopolymerization scheme based on the procedure suggested by Estenoz et al.[34], allows the calculation of the cumulative SAN grafting efficiency, the number chain length distribution (NCLD) of the non-grafted SAN, and the average composition of the non-grafted SAN. This procedure is based on recurrent molar balances of macroradicals as a function of their length, using the pseudo-stationary state assumption for all of the radical species.[34] Differential Equation (B18)–(B20), (B25)–(B26) and (B29) were solved through a finite difference method, employing the same time intervals as obtained from the integration of the balances in Appendix A. In order to avoid extremely high computational times, a simplified method that calculates a reduced number of (fictitious) species was applied to solve Equation (B29).[33–37] To this purpose, the distribution was discretized by adopting 1 000 species, lumping together all species that fall within a fixed chain-length interval of 250 comonomer units. Finally, the cumulative SAN grafting efficiency, average compositions of non-grafted SAN, and average molecular weights of the non-grafted SAN were calculated through Equation (B24), (B27)–(B28) and (B35)–(B38), respectively.

Even though results corresponding to a simpler homogeneous model are presented in this article, it is not further

Table 3. Kinetic parameters at 80 °C.

Parameter	Value	Reference
k_d [s^{-1}]	4.0914×10^{-5}	[59]
k_{i0} [$L^2 \cdot mol^{-2} \cdot s^{-1}$]	1.4971×10^{-12}	[37]
f [−]	0.57	[59]
k_{is}, k_{pss}, k_{bs} [$L \cdot mol^{-1} \cdot s^{-1}$]	469.1345	[37,56]
$r_1 = k_{pss}/k_{psa}$ [−]	0.36	[56]
k_{ia}, $k_{ba} = k_{psa}$ [$L \cdot mol^{-1} \cdot s^{-1}$]	k_{pss}/r_1	[56]
k_{ib} [$L \cdot mol^{-1} \cdot s^{-1}$]	83.76	[37]
k_{paa} [$L \cdot mol^{-1} \cdot s^{-1}$]	5.6460×10^5	[56]
$r_2 = k_{paa}/k_{pas}$ [−]	0.078	[56]
k_{pas} [$L \cdot mol^{-1} \cdot s^{-1}$]	k_{paa}/r_2	[56]
k_{fss} [$L \cdot mol^{-1} \cdot s^{-1}$]	0.0328	[56]
k_{fsa} [$L \cdot mol^{-1} \cdot s^{-1}$]	0.9871	[56]
k_{faa} [$L \cdot mol^{-1} \cdot s^{-1}$]	11.2185	[56]
k_{fas} [$L \cdot mol^{-1} \cdot s^{-1}$]	55.8899	[56]
k_{fsb} [$L \cdot mol^{-1} \cdot s^{-1}$]	0.5207	[37]
k^0_{tss}, k^0_{tbs} [$L \cdot mol^{-1} \cdot s^{-1}$]	1.1487×10^8	[56]
k^0_{taa} [$L \cdot mol^{-1} \cdot s^{-1}$]	1.4359×10^9	[56]
k^0_{tsa}, k^0_{tba} [$L \cdot mol^{-1} \cdot s^{-1}$][a)]	$32\frac{\{0.0625(1-\psi^0_S)+0.36\psi^0_S\}}{1-\psi^0_S+0.36\psi^0_S}\sqrt{k^0_{tss}k^0_{taa}}$	[56]

[a)] ψ^0_S is the molar fraction of S in the initial mixture of comonomers.

explained in this section. This is because homogeneous model represents a particular case of this heterogeneous version, where phase separation is not imposed and a single SB-rich phase is considered along the complete polymerization.

Simulated Results

Model Adjustment

Consider the adjustment of the new model to Reaction A. Reaction B will be considered for the model validation. Most of the model kinetic parameters were directly taken from literature, and they are presented in Table 3. The other required parameters are reported in Table 4 and 5. Since the rubber microstructure strongly affects the grafting reactions,[45,47] the rate constants of chemical initiation of butadiene units and the rate constant of chain transfer from styryl macroradicals to B were adopted from the heterogeneous model by Luciani,[37] that involved a rubber with essentially the same microstructure as the one used in this work. Rate constants of S thermal initiation in

Table 5. Adjusted parameters.

Model	A	k_{fab}
		$L \cdot mol^{-1} \cdot s^{-1}$
homogeneous	0.720	3.9127×10^3
heterogeneous, $K_I = 1$	0.630	1.4644×10^4
heterogeneous, $K_I = 2$	0.697	1.0899×10^4
heterogeneous, $K_I = 3$	0.780	9.5573×10^3

Table 4. Other parameters of the model at 80 °C.

Parameter	Value	Reference
Thermal expansion coefficients [K^{-1}]:		
α_{SAN}	2.50×10^{-4}	[56]
α_{PB}	4.49×10^{-4}	[60]
α_{PS}	3.65×10^{-4}	[56]
α_{S}	6.40×10^{-4}	[56]
α_{AN}	1.25×10^{-3}	[56]
Glass transition temperatures [K]:		
$T_{g,PB}$	188.1	[61]
$T_{g,PS}$	373.2	[62]
$T_{g,S}$	185.2	[56]
$T_{g,AN}$	190.4	[56]
$T_{g,PAN}$	378.2	[62]
$T_{g,SANalt}$	384.7	[62]
$T_{g,SAN}$ [a]	$\theta_S T_{g,PS} + (1-\theta_S) T_{g,PAN} + R_t/100 (T_{g,SANalt} - \overline{T}_{g,SAN})$	[62]
	$R_t = 400(1-\theta_S)\theta_S / \{1 + [1 + 4\theta_S(1-\theta_S)(r_1 r_2 - 1)]^{1/2}\}$	[62]
	$\overline{T}_{g,SAN} = (T_{g,PAN} + T_{g,PS})/2$	[62]
Densities [$kg \cdot m^{-3}$]:		
ρ_{PB}	864.2	[63]
ρ_{PS}	1036.3	[63]
ρ_{S}	850.12	[64]
ρ_{AN}	758.46	[65]
ρ_{I}	1202.0	[65]
ρ_{PAN}	1175.0	[63,60]
ρ_{SAN} [b]	$[\overline{w}_S/\rho_{PS} + (1-\overline{w}_S)/\rho_{PAN}]^{-1}$	–

[a] θ_s is the cumulative molar fraction of S in the SAN copolymer; [b] $\overline{w}_s$ is the cumulative weight fraction of S repeat units of the SAN copolymer.

Macromol. Theory Simul. **2008**, *17*, 180–197

Macromolecular Journals
DOI: 10.1002/mats.200800004

Reaction (R2), S chemical initiation in Reaction (R3), and S homopropagation in Reaction (R8) were also adopted from Luciani.[37] According to previous publications on the bulk HIPS process,[34–37] the rate constants for the S chemical initiation in Reaction (R3) and for the primary addition of S to B$^\bullet$ in Reaction (R6) were assumed to be equal to the rate constant of S homopropagation in Reaction (R8). The termination rate constant between B$^\bullet$ and S-ended macroradicals in Reaction (R38) and (R40) was assumed to be equal to the termination rate constant between S-ended macroradicals in Reaction (R28) and (R35). Similarly, the rate constant for AN chemical initiation in Reaction (R4) and primary addition of AN to B$^\bullet$ in Reaction (R7), were assumed to be equal to the rate constant of the propagation of S$^\bullet$ with AN in Reaction (R9); and the termination rate constant between B$^\bullet$ and AN-ended macroradicals in Reaction (R39) and (R41) was assumed to be equal to the rate constant of termination between S-ended macroradicals and AN-ended macroradicals in Reaction (R29), (R32), (R33) and (R36).

Due to the lack of experimental studies involving S/AN/SAN/SB blends, the following approximations related to the system thermodynamics were adopted: a) the phase separation takes place at 2% conversion (a typical value for the bulk HIPS process);[16,37,38,40] and, b) the partition coefficients of the low molar mass species are constant along the reaction. Based on the experimental work by Locatelli and Riess,[42] it was assumed that comonomers were evenly distributed between phases, with $K_S = K_{AN} = 1$. Three (fixed) scenarios were adopted for the distribution of BPO initiator between the phases: strong, moderate and no initiator preference for the SB-rich phase, setting K_I to 3, 2, and 1, respectively.

The performance of the homogeneous and heterogeneous models for fitting the measurements was evaluated. The rate constant of transfer reaction from an AN-ended macroradical to B (k_{fab}) in Reaction (R25) and (R27) and the parameter A in Equation (3) were sequentially adjusted to fit the conversion and the cumulative SAN grafting efficiency of Reaction A. The adjustment was carried out minimizing the absolute average deviation between measurements and simulation results. Parameter A was first calculated by minimizing the deviation in the comonomers conversion. With the resulting value of A, k_{fab} was estimated by minimizing the deviation in the SAN grafting efficiency. Minimizations were carried out through an iterative numerical method, and the parameters are presented in Table 5. Comparing the different heterogeneous scenarios, a higher K_I causes higher radical concentration in the SB-rich phase, and the value of k_{fab} must drop to attain the same level of grafting.

Table 6 shows the average absolute deviation of conversion (x), SAN grafting efficiency (E_{SAN}), and average molecular weights of the non-grafted SAN ($\overline{M}_{n,ngSAN}$ and $\overline{M}_{w,ngSAN}$). Figure 1–4 present the model results and experimental data, while Figure 6–8 present some additional theoretical results. As shown in Table 6, the cumulative SAN grafting efficiency is quite considerably affected by the model scenario. For this reason, Figure 2 includes all the model results and it is observed the best fit is obtained when BPO partition coefficient is set to 1. The other figures only show predictions corresponding to the heterogeneous model with $K_I = 1$. For this last model, and based on the error bands from experimental techniques, the following confidence limits were calculated for the adjusted parameters: $A = 0.630 \pm 0.116$ and $k_{fab} = 1.4644 \times 10^4 \pm 2.226 \times 10^3$ L · mol^{-1} · s^{-1}.

Discussion

Consider first the simulation results of the conversion, average molecular weights, and average composition of non-grafted SAN of Figure 1, 3, and 4.

Conversions with and without considering the gel effect are shown in Figure 1a and b, respectively. As expected for

Table 6. Average absolute deviation from experimental values of some simulated variables.

Reaction	Variable	Homogeneous Model	Heterogeneous Model		
			$K_I = 1$	$K_I = 2$	$K_I = 3$
A	x [%]	0.936	0.928	0.932	0.928
	E_{SAN} [%]	2.785	0.718	0.856	0.964
	$\overline{M}_{n,ngSAN}$ [g · mol^{-1}]	8 495	10 589	9 306	8 534
	$\overline{M}_{w,ngSAN}$ [g · mol^{-1}]	26 121	20 999	21 262	21 338
B	x [%]	0.592	0.726	0.630	0.632
	E_{SAN} [%]	6.162	1.131	2.189	2.621
	$\overline{M}_{n,ngSAN}$ [g · mol^{-1}]	32 199	20 679	22 454	23 090
	$\overline{M}_{w,ngSAN}$ [g · mol^{-1}]	58 222	27 040	29 708	30 471

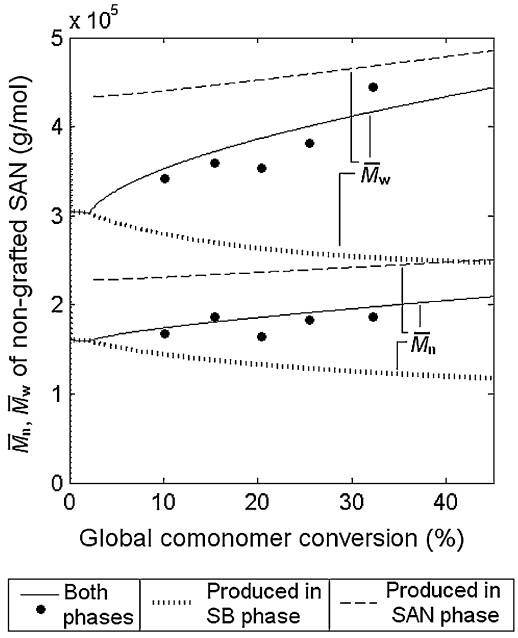

Figure 6. Number- and weight-average molecular weights of the total non-grafted SAN, non-grafted SAN produced in the SB-rich phase, and non-grafted SAN produced in the SAN-rich phase for Reaction A. Experimental data are represented by symbols and simulation results from the heterogeneous model with $K_I = 1$ are represented by traces.

bulk SAN polymerizations,[53–56] the gel effect is important even at low conversions.

Since graft polymers generated along HIPS and ABS processes are the main responsible for the interfacial tension reduction and for the development of the rubber particle morphology,[15–17,37] feasible morphological models will require a precise knowledge of the evolution of the grafting extent. The homogeneous model predicts an increasing SAN grafting efficiency, in contradiction to the experimental data (see Figure 2a). This can be explained in terms of the generation of butadienyl radicals B•, produced via either chemical initiation or transfer to the rubber. Along the homogeneous stage, the concentration of B units remains essentially constant because the reaction volume and the unreacted B units concentration remain almost constant, while the comonomers concentration is strongly reduced. This promotes the generation of grafted macroradicals with respect to the non-grafted copolymer radicals, increasing the SAN grafting efficiency. Figure 2b–d show the results of the heterogeneous model for the 3 different partition coefficients of BPO. Similarly to the homogeneous model, the heterogeneous model predicts an increasing grafting efficiency until phase separation point at $x = 2\%$. After this point however, a continuous decrease is observed, in accord with experimental results. The decrease in the grafting efficiency comes from a reduction of the length of SAN branches attached to the graft terpolymer, as a consequence of the increase of B concentration in the SB-rich phase, and the corresponding increase of the rate of chain transfers to the rubber.

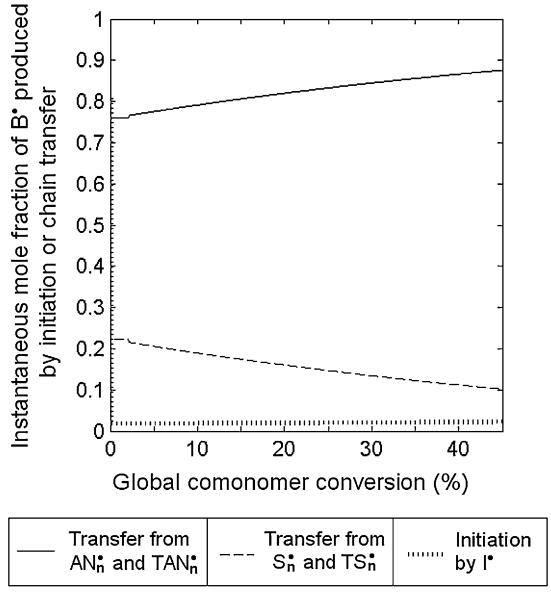

Figure 7. Fractional contribution of different reactions for the instantaneous production of B• in Reaction A of the heterogeneous model with $K_I = 1$.

Although average molar masses were not considered for the model adjustment, a reasonable agreement with experimental results is obtained for both reactions (see Figure 3). The increasing molar mass of the total non-grafted SAN is a combination of a fraction (of decreasing volume and relatively low molecular weight) produced in the SB-rich phase and a fraction (of increasing volume and relatively high molecular weight) produced in the SAN-rich phase (Figure 6). Since transfer reactions to the rubber do not occur in the SAN-rich phase, the non-grafted SAN produced there exhibits higher molar masses. Even though they are not shown here for space reasons, the calculated molecular weights of the grafted SAN are almost equal to those of the non-grafted SAN produced in the SB-rich phase. Unfortunately, this last result could not be compared with measurements because the isolation of the SAN branches from the mixture of graft copolymers and unreacted SB was not performed.

Consider the simulation results in Figure 4 for the non-grafted SAN chemical composition. Predictions of both reactions are overlapping, and the non-grafted SAN composition remains essentially constant and equal to the comonomers feed ratio. Also, it is independent of the initiator partition. This is due to comonomer consumption being assumed only as a function of the propagation reactions, in which case, SAN composition is governed by the comonomer ratio. In turn, the comonomer ratio is constant along prepolymerization because K_{AN} and K_S are

Macromol. Theory Simul. **2008**, *17*, 180–197

Macromolecular Journals
DOI: 10.1002/mats.200800004

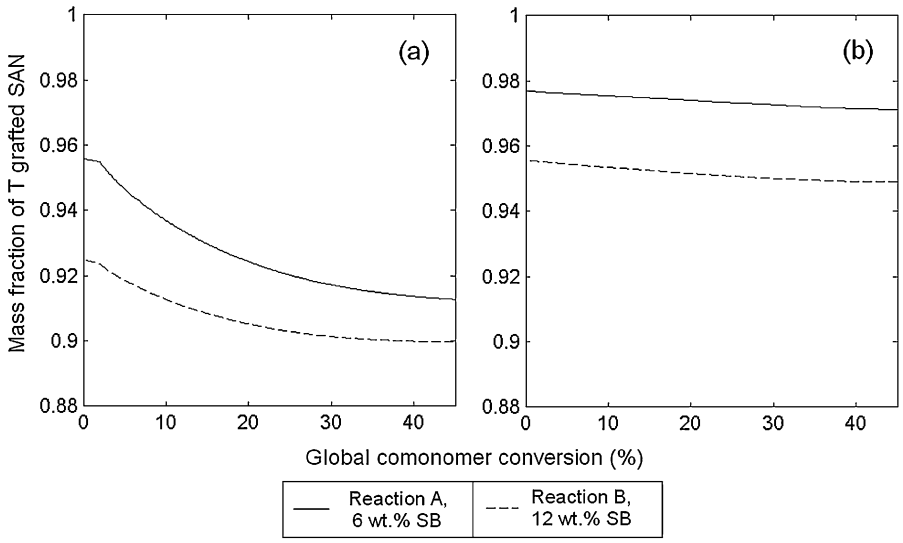

Figure 8. Simulated mass fraction of T-shaped SAN branches as a function of global comonomer conversion. a) Heterogeneous model with $K_I = 1$, b) homogeneous model.

set to 1, the comonomer feed composition is close to the theoretical azeotropic point, and the investigated conversions are low. Under such conditions, it can be proven that the composition of grafted and non-grafted SAN produced in both phases is strictly the same.

Regarding the relative importance of initiation or chain transfer reactions to produce grafted macroradicals, it was theoretically verified that in this model most of the grafting comes from the chain transfer reaction from AN-ended macroradicals towards the B repeating units (Figure 7).

Figure 8a shows the fraction of T-shaped branches in the terpolymer calculated from the heterogeneous model with $K_I = 1$. It predicts that more than 90% of grafted SAN branches are T-shaped. As expected, this fraction is reduced as the conversion increases due to the increasing [B]/([AN] + [S]) ratio. Compared with the heterogeneous model predictions, the homogeneous model underestimates the H-shaped branches content (see Figure 8b). This is because the homogeneous assumption considers a considerable lower [B]/([AN] + [S]) ratio.

Conclusion

A novel mathematical model was developed for the copolymerization of S and AN in the presence of SB. Even though a simple homogeneous model is able to adequately predict conversion, molar masses and composition of non-grafted SAN, higher deviations are expected when predicting variables related with the generated graft terpolymer (i.e., grafting efficiency, type of SAN grafted branches, molar masses, etc.). For 4 different model scenarios, 2 parameters were adjusted: the rate constant of chain transfer reaction from AN-ended macroradicals to butadiene repeating units and a constant that considers the gel effect. Although BPO partition showed a relatively minor effect on the simulations, the best results were obtained for the heterogeneous model with BPO evenly distributed between phases.

Appendix A: Global Module

Consider first the global balances of species in a batch reactor that produces ABS. Brackets indicate the molar concentration, subscript j denotes each of the phases (with $j = 1$ for the SB-rich phase and $j = 2$ for the SAN-rich phase) and no subscript indicates total molar concentration.

Initiator

$$\frac{d([I]V)}{dt} = -\sum_{j=1,2} k_d [I]_j V_j \tag{A1}$$

$$[I]_1 = K_I [I]_2 \tag{A2}$$

where V is the total volume of the reaction mixture, V_j is the volume of the phase j, and K_I is the partition coefficient of the initiator.

Comonomers

Assuming long chain approximation (by which comonomers are only consumed in the propagation reactions), the following balances are derived:

$$\frac{d([S]V)}{dt} = -\sum_{j=1,2}[S]_j(k_{pss}[S^\bullet]_j + k_{pas}[AN^\bullet]_j + k_{pss}[TS^\bullet]_j + k_{pas}[TAN^\bullet]_j)V_j \quad (A3)$$

$$[S]_1 = K_S[S]_2 \quad (A4)$$

$$\frac{d([AN]V)}{dt} = -\sum_{j=1,2}[AN]_j(k_{paa}[AN^\bullet]_j + k_{psa}[S^\bullet]_j + k_{paa}[TAN^\bullet]_j + k_{psa}[TS^\bullet]_j)V_j \quad (A5)$$

Unreacted Butadiene Units

$$\frac{d([B]_1V_1)}{dt} = -[B]_1\{k_{ib}[I^\bullet]_1 + k_{fsb}([S^\bullet]_1 + [TS^\bullet]_1) + k_{fab}([AN^\bullet]_1 + [TAN^\bullet]_1)\}V_1 \quad (A7)$$

Radicals

$$\frac{d([I^\bullet]_jV_j)}{dt} = \{2fk_d[I]_j - [I^\bullet]_j(k_{is}[S]_j + k_{ia}[AN]_j + k_{ib}[B]_j)\}V_j \quad j = 1,2 \quad (A8)$$

$$\frac{d([S^\bullet]_jV_j)}{dt} = \{2k_{i0}[S]_j^3V_j + [S]_j\{k_{is}[I^\bullet]_j + (k_{pas} + k_{fas})[AN^\bullet]_j + k_{fss}[TS^\bullet]_j + k_{fas}[TAN^\bullet]_j\}V_j - [S^\bullet]_j\{(k_{psa} + k_{fsa})[AN]_j + k_{fsb}[B]_j + k_{tssj}([S^\bullet]_j + [TS^\bullet]_j) + k_{tsaj}([AN^\bullet]_j + [TAN^\bullet]_j) + k_{tbsj}[B^\bullet]_j\}V_j \quad j = 1,2 \quad (A9)$$

$$\frac{d([AN^\bullet]_jV_j)}{dt} = [AN]_j\{k_{ia}[I^\bullet]_j + (k_{psa} + k_{fsa})[S^\bullet]_j + k_{faa}[TAN^\bullet]_j + k_{fsa}[TS^\bullet]_j\}V_j - [AN^\bullet]_j\{(k_{pas} + k_{fas})[S]_j + k_{fab}[B]_j + k_{taaj}([AN^\bullet]_j + [TAN^\bullet]_j) + k_{tsaj}([S^\bullet]_j + [TS^\bullet]_j) + k_{tbaj}[B^\bullet]_j\}V_j \quad j = 1,2 \quad (A10)$$

$$\frac{d([TS^\bullet]_1V_1)}{dt} = [S]_1\{k_{bs}[B^\bullet]_1 + k_{pas}[TAN^\bullet]_1\}V_1 - [TS^\bullet]_1\{(k_{psa} + k_{fsa})[AN]_1 + k_{fss}[S]_1 + k_{fsb}[B]_1 + k_{tss1}([S^\bullet]_1 + [TS^\bullet]_1) + k_{tsa1}([AN^\bullet]_1 + [TAN^\bullet]_1) + k_{tbs1}[B^\bullet]_1\}V_1 \quad (A11)$$

$$\frac{d([TAN^\bullet]_1V_1)}{dt} = [AN]_1\{k_{ba}[B^\bullet]_1 + k_{psa}[TS^\bullet]_1\}V_1 - [TAN^\bullet]_1\{(k_{pas} + k_{fas})[S]_1 + k_{faa}[AN]_1 + k_{fab}[B]_1 + k_{taa1}([AN^\bullet]_1 + [TAN^\bullet]_1) + k_{tsa1}([S^\bullet]_1 + [TS^\bullet]_1) + k_{tba1}[B^\bullet]_1\}V_1 \quad (A12)$$

$$\frac{d([B^\bullet]_1V_1)}{dt} = [B]_1\{k_{ib}[I^\bullet]_1 + k_{fsb}([S^\bullet]_1 + [TS^\bullet]_1) + k_{fab}([AN^\bullet]_1 + [TAN^\bullet]_1)\}V_1 - [B^\bullet]_1\{k_{bs}[S]_1 + k_{ba}[AN]_1 + k_{tbs1}([S^\bullet]_1 + [TS^\bullet]_1) + k_{tba1}([AN^\bullet]_1 + [TAN^\bullet]_1)\}V_1 \quad (A13)$$

$$[AN]_1 = K_{AN}[AN]_2 \quad (A6)$$

where $[S^\bullet]_j = \sum_{n=1}^{\infty}[S_n^\bullet]_j$, $[AN^\bullet]_j = \sum_{n=1}^{\infty}[AN_n^\bullet]_j$, $[TS^\bullet]_j = \sum_{n=1}^{\infty}[TS_n^\bullet]_j$, and $[TAN^\bullet]_j = \sum_{n=1}^{\infty}[TAN_n^\bullet]_j$ are the total radical concentrations in each phase; and K_S and K_{AN} are the partition coefficients of the comonomers.

Phase Volumes

During the initial homogeneous stage before phase separation, the following expression is employed to estimate the variation of the single SB-rich phase volume (V_1):

$$\frac{dV_1}{dt} = -V_1\{([S^\bullet]_1 + [TS^\bullet]_1)(k_{pss}[S]_1M_S(1/\rho_S - 1/\rho_{PS}) + k_{psa}[AN]_1M_{AN}(1/\rho_{AN} - 1/\rho_{PAN}) + ([AN^\bullet]_1 + [TAN^\bullet]_1)(k_{pas}[S]_1M_S(1/\rho_S - 1/\rho_{PS}) + k_{paa}[AN]_1M_{AN}(1/\rho_{AN} - 1/\rho_{PAN})\} \quad (A14)$$

Macromol. Theory Simul. 2008, 17, 180–197

Macromolecular Journals
DOI: 10.1002/mats.200800004

After the phase separation point, the following expressions are used to estimate the volumes of the 2 coexisting phases:

$$V_1 = \left\{ \frac{\overline{w}^0_{S,SB} m^0_{SB}}{\rho_{PS}} + \frac{(1-\overline{w}^0_{S,SB}) m^0_{SB}}{\rho_{PB}} \right\} \Big/ \left\{ 1 - \left(\frac{[S]_1 M_S}{\rho_S} + \frac{[AN]_1 M_{AN}}{\rho_{AN}} + \frac{[I]_1 M_I}{\rho_I} \right) \right\} \quad \text{(A15)}$$

$$V_2 = \left\{ \frac{m^0_S - [S] M_S V}{\rho_{PS}} + \frac{m^0_{AN} - [AN] M_{AN} V}{\rho_{PAN}} \right\} \Big/ \left\{ 1 - \left(\frac{[S]_2 M_S}{\rho_S} + \frac{[AN]_2 M_{AN}}{\rho_{AN}} + \frac{[I]_2 M_I}{\rho_I} \right) \right\} \quad \text{(A16)}$$

where m^0_S, m^0_{AN}, and m^0_{SB} are the initial masses of S, AN, and SB, respectively; $\overline{w}^0_{S,SB}$ is the average weight content of S in the initial SB; M_i (i = S, AN, I) is the molar mass of species I; and ρ_i is the density of species (i = S, AN, I, PS, PAN, PB). Note that volume of SAN has been calculated from the volumes of its polystyrene and polyacrylonitrile (PAN) fractions.

Global Comonomer Conversion

$$x = \frac{m^0_S + m^0_{AN} - ([S] M_S + [AN] M_{AN}) V}{m^0_S + m^0_{AN}} \quad \text{(A17)}$$

Appendix B: Pseudo-Homopolymerization Module

The S and AN copolymerization is assumed here as a pseudo-homopolymerization. This approximation allows the approach of Estenoz et al.[34] to be used to calculate the cumulative grafting efficiency, the NCLD of the non-grafted SAN, the amounts of T- and H-shaped branches of SAN in SB-*g*-SAN, and the AN content in the non-grafted SAN.

Consider first some definitions. From the global concentrations of species calculated in Appendix A, the total comonomers concentration $[M]_j$, total non-grafted macroradicals concentration $[C^\bullet]_j$, and total grafted radicals concentration $[T^\bullet]_j$ can be calculated, as follows:

$$[M]_j = [S]_j + [AN]_j \quad j = 1,2 \quad \text{(B1)}$$

$$[C^\bullet]_j = [AN^\bullet]_j + [S^\bullet]_j \quad j = 1,2 \quad \text{(B2)}$$

$$[T^\bullet]_j = [TAN^\bullet]_j + [TS^\bullet]_j \quad j = 1,2 \quad \text{(B3)}$$

Also, the following global rate constants of propagation ($k_{p,j}$), chain transfer to the comonomers ($k_{fm,j}$), chain transfer to the rubber ($k_{fb,j}$), termination by recombination of copolymer radicals ($k_{t,j}$), and termination by recombination between butadienyl and copolymer radicals ($k_{tb,j}$) are defined in each phase.

$$k_{p,j} = k_{paa} z_j w_j + k_{psa}(1-w_j) z_j + k_{pas} w_j (1-z_j) + k_{pss}(1-w_j)(1-z_j) \quad j = 1,2 \quad \text{(B4)}$$

$$k_{fm,j} = k_{faa} w_j z_j + k_{fas} w_j (1-z_j) + k_{fss}(1-w_j)(1-z_j) + k_{fsa}(1-w_j) z_j \quad j = 1,2 \quad \text{(B5)}$$

$$k_{fb,j} = k_{fsb}(1-w_j) + k_{fab} w_j \quad j = 1,2 \quad \text{(B6)}$$

$$k_{t,j} = k_{taa,j} w_j^2 + 2k_{tsa,j}(1-w_j) w_j + k_{tss,j}(1-w_j)^2 \quad j = 1,2 \quad \text{(B7)}$$

where w_j and z_j are the radical and comonomer concentration ratios, given by:

$$w_j = \frac{[AN^\bullet]_j}{[C^\bullet]_j} = \frac{[TAN^\bullet]_j}{[T^\bullet]_j} \quad j = 1,2 \quad \text{(B8)}$$

$$z_j = \frac{[AN]_j}{[M]_j} \quad j = 1,2 \quad \text{(B9)}$$

The global rate of comonomers consumption in each phase $R_{p,j}$ is calculated as follows:

$$R_{p,j} = k_{p,j} [M]_j ([C^\bullet]_j + [T^\bullet]_j) \quad j = 1,2 \quad \text{(B10)}$$

From Reaction (R16–R41) in Table 2, let us define the following probabilities of a consumed comonomer for reacting to produce a non-grafted SAN chain ($P_{ngSAN,j}$), a

T-shaped SAN branch ($P_{gSANT,j}$), or a H-shaped SAN branch ($P_{gSANH,j}$):[34]

$$P_{p\,ngSAN,j} = \varphi_j \frac{k_{fm,j}[M]_j + k_{fb,j}[B]_j + k_{t,j}[C^\bullet]_j}{k_{fm,j}[M]_j + k_{fb,j}[B]_j + k_{t,j}([C^\bullet]_j + [T^\bullet]_j) + k_{tb,j}[B^\bullet]_j} \quad j = 1,2 \tag{B11}$$

$$P_{p\,gSANT,j} = \frac{\varphi_j(k_{t,j}[T^\bullet]_j + k_{tb,j}[B^\bullet]_j) + (1-\varphi_j)(k_{fm,j}[M]_j + k_{fb,j}[B]_j + k_{t,j}[C^\bullet]_j)}{k_{fm,j}[M]_j + k_{fb,j}[B]_j + k_{t,j}([C^\bullet]_j + [T^\bullet]_j) + k_{tb,j}[B^\bullet]_j} \quad j = 1,2 \tag{B12}$$

$$P_{p\,gSANH,j} = (1-\varphi_j) \frac{k_{t,j}[T^\bullet]_j + k_{tb,j}[B^\bullet]_j}{k_{fm,j}[M]_j + k_{fb,j}[B]_j + k_{t,j}([C^\bullet]_j + [T^\bullet]_j) + k_{tb,j}[B^\bullet]_j} \quad j = 1,2 \tag{B13}$$

where:

$$\varphi_j = \frac{[C^\bullet]_j}{[C^\bullet]_j + [T^\bullet]_j} \quad j = 1,2 \tag{B14}$$

From these probabilities, $R_{p,j}$ can be subdivided into the comonomer consumption rates to produce non-grafted SAN ($R_{p\,ngSAN,j}$), T-shaped SAN branches ($R_{p\,gSANT,j}$), or H-shaped SAN branches ($R_{p\,gSANH,j}$), as follows:

$$R_{p\,ngSAN,j} = R_{p,j} P_{ngSAN,j} \tag{B15}$$

$$R_{p\,gSANT,j} = R_{p,j} P_{gSANT,j} \tag{B16}$$

$$R_{p\,gSANH,j} = R_{p,j} P_{gSANH,j} \tag{B17}$$

The total balances of the masses of non-grafted SAN ($G_{ngSAN,j}$), T-shaped SAN branches ($G_{gSANT,j}$), and H-shaped SAN branches ($G_{gSANH,j}$) in each phase can be estimated through:

$$\frac{d(G_{ngSAN,j})}{dt} = R_{p\,ngSAN,j} V_j M_{SAN,j} \quad j = 1,2 \tag{B18}$$

$$\frac{d(G_{gSANT,j})}{dt} = R_{p\,gSANT,j} V_j M_{SAN,j} \quad j = 1,2 \tag{B19}$$

$$\frac{d(G_{gSANH,j})}{dt} = R_{p\,gSANH,j} V_j M_{SAN,j} \quad j = 1,2 \tag{B20}$$

where $M_{SAn,j}$ represents the instantaneous average molecular weight of a SAN repeating units in each phase, that in turn is calculated as follows:

$$M_{SAN,j} = \frac{R_{ps,j} M_S + R_{pa,j} M_{AN}}{R_{ps,j} + R_{pa,j}} \quad j = 1,2 \tag{B21}$$

where $R_{ps,j}$ and $R_{pa,j}$ are the rates of S and AN consumption; and $R_{ps,j}$ and $R_{pa,j}$ are calculated through the following expressions:

$$R_{ps,j} = [S]_j\{k_{pss}([S^\bullet]_j + [TS^\bullet]_j) + k_{pas}([AN^\bullet]_j + [TAN^\bullet]_j)\} \quad j = 1,2 \tag{B22}$$

$$R_{pa,j} = [AN]_j\{k_{paa}([AN^\bullet]_j + [TAN^\bullet]_j) + k_{psa}([S^\bullet]_j + [TS^\bullet]_j)\} \quad j = 1,2 \tag{B23}$$

Cumulative SAN Grafting Efficiency

$$E_{SAN} = \frac{\sum_{j=1,2}(G_{gSANT,j} + G_{gSANH,j})}{\sum_{j=1,2}(G_{gSANT,j} + G_{gSANH,j} + G_{ngSAN,j})} \tag{B24}$$

Average AN Content in the Non-Grafted SAN

The masses of S ($S_{ngSAN,j}$) and AN ($AN_{ngSAN,j}$) contained in the accumulated non-grafted SAN are estimated through the following balances:

$$\frac{d(S_{ngSAN,j})}{dt} = R_{ps,j} P_{ngSAN,j} V_j \quad j = 1,2 \tag{B25}$$

$$\frac{d(AN_{ngSAN,j})}{dt} = R_{pa,j} P_{ngSAN,j} V_j \quad j = 1,2 \tag{B26}$$

The average content of AN in the non-grafted SAN produced in each phase ($\overline{w}_{AN,ngSAN,j}$), and in the total non-grafted SAN ($\overline{w}_{AN,ngSAN}$) are calculated as follows:

$$\overline{w}_{AN,ngSAN,j} = \frac{AN_{ngSAN,j} M_{AN}}{AN_{ngSAN,j} M_{AN} + S_{ngSAN,j} M_S} \tag{B27}$$

$$\overline{w}_{AN,ngSAN} = \frac{\sum_{j=1,2} AN_{ngSAN,j} M_{AN}}{\sum_{j=1,2}(AN_{ngSAN,j} M_{AN} + S_{ngSAN,j} M_S)} \tag{B28}$$

Macromol. Theory Simul. 2008, 17, 180–197

Macromolecular Journals
DOI: 10.1002/mats.200800004

Number Chain Length Distribution of the Non-Grafted SAN

Following the work by Estenoz et al.[34], the cumulative NCLD of non-grafted SAN produced in each phase is obtained through the following species balances:

$$\frac{d\{[C_n]_j V_j\}}{dt} = R_{p,j} V_j \varphi_j \left[\tau_j - \gamma_j \tau_{1j} + \frac{1}{2}\beta_j \varphi_j \alpha_j n\right] \alpha_j e^{-\alpha_j n} \quad n = 2, 3, \ldots, \infty \quad j = 1, 2 \tag{B29}$$

where:

$$\beta_j = \frac{k_{t,j} R_{p,j}}{(k_{p,j}[M]_j)^2} \quad j = 1, 2 \tag{B30}$$

$$\tau_j = \frac{k_{fm,j}}{k_{p,j}} + \frac{k_{fb,j}[B]_j}{k_{p,j}[M]_j} + \gamma_j \tau_{1j} \quad j = 1, 2 \tag{B31}$$

$$\tau_{1j} = \frac{k_{tb,j} R_{p,j}}{(k_{p,j}[M]_j)^2} \quad j = 1, 2 \tag{B32}$$

$$\gamma_j = \frac{[B^\bullet]_j}{[C^\bullet]_j + [T^\bullet]_j} \quad j = 1, 2 \tag{B33}$$

$$\alpha_j = \tau_j + \beta_j \quad j = 1, 2 \tag{B34}$$

Average Molar Masses of Non-Grafted SAN

Since experimental conditions do not tend to produce copolymer compositional drift, the molecular weight of a SAN repeating units is estimated from Equation (B21), and the following averages molar masses are estimated for the non-grafted SAN:

$$\overline{M}_{n,ngSAN,j} = M_{SAN,j} \frac{\sum_{n=1}^{\infty} [C_n]_j n}{\sum_{n=1}^{\infty} [C_n]_j}; \quad j = 1, 2 \tag{B35}$$

$$\overline{M}_{w,ngSAN,j} = M_{SAN,j} \frac{\sum_{n=1}^{\infty} [C_n]_j n^2}{\sum_{n=1}^{\infty} [C_n]_j n}; \quad j = 1, 2 \tag{B36}$$

The average molar masses of the total non-grafted SAN are calculated through:

$$\overline{M}_{n,ngSAN} = \frac{\sum_{j=1,2} \sum_{n=1}^{\infty} [C_n]_j n\, M_{SAN,j} V_j}{\sum_{j=1,2} \sum_{n=1}^{\infty} [C_n]_j V_j} \tag{B37}$$

$$\overline{M}_{w,ngSAN} = \frac{\sum_{j=1,2} \sum_{n=1}^{\infty} [C_n]_j n^2\, M_{SAN,j} V_j}{\sum_{j=1,2} \sum_{n=1}^{\infty} [C_n]_j n V_j} \tag{B38}$$

Nomenclature

A	Constant parameter related to the gel effect
AN	Acrylonitrile
$AN_1^\bullet$	Primary acrylonitrile radical
$AN_n^\bullet$	AN-ended non-primary copolymer radical with n comonomer repeating units
B	Butadiene repeating units in SB
$B^\bullet$	Primary radical of B
C_n	SAN copolymer with n comonomer repeating units
E_{SAN}	Cumulative SAN grafting efficiency
f	Initiator efficiency
H_n	H-shaped SAN branch with n comonomer repeating units
I	Initiator
$I^\bullet$	Primary initiator radical
K_i	Partition coefficient of species i (i = S, AN, I)
m_{ngSAN}	Mass of non-grafted SAN contained in a mixture of unreacted SB and SB-g-SAN
m_p	Mass of polymer contained in a sample
m_s	Mass of a sample
$\overline{M}_{n,ngSAN}$	Number-average molar mass of the non-grafted SAN
$\overline{M}_{w,ngSAN}$	Weight-average molar mass of the non-grafted SAN
PAN	Poly(acrylonitrile)
PS	Polystyrene
PB	Polybutadiene
r_1, r_2	Homopropagation to crosspropagation reactivity ratios
S	Styrene monomer
$S_1^\bullet$	Primary styrene radical
$S_n^\bullet$	S-ended non-primary copolymer radical with n comonomer repeating units
SB	Styrene-butadiene block copolymer
T_n	T-shaped SAN branch with n comonomer repeating units
$TAN_1^\bullet$	Primary terpolymer radical generated by addition of AN onto $B^\bullet$
$TAN_n^\bullet$	AN-ended non-primary terpolymer radical with n comonomer repeating units
$T_{g,I}$	Glass transition temperature of species i (i = S, AN, PS, PB, PAN)
$\overline{T}_{g,SAN}$	Average glass transition temperature of SAN
$T_{g,SANalt}$	Glass transition temperature of a strictly alternating SAN

$TS_1^{\bullet}$	Primary terpolymer radical generated by addition of S onto $B^{\bullet}$
$TS_n^{\bullet}$	S-ended non-primary terpolymer radical with n comonomers repeating units
V	Volume
V_f	Free volume
V_f^{Cr}	Critical free volume
$\overline{w}_{AN,ngSAN}$	Average content of AN in the non-grafted SAN
w_{SB}	Weight fraction of SB
x	Comonomer conversion

Greek Symbols

α_i	Difference in the thermal expansion coefficient of species i (i = S, AN, PS, PB, SAN) above and below $T_{g,i}$
ϕ_i	Volume fraction of species i (i = S, AN, PS, PB, SAN)
θ_s	Cumulative molar fraction of S in the SAN copolymer
ρ_i	Mass density of species i (i = S, AN, PS, PB, PAN, SAN)
ψ_s	Molar fraction of S in the comonomer mixture

Superscript

0	Initial condition

Subscripts

1	SB-rich phase
2	SAN-rich phase

Received: January 19, 2008; Revised: February 18, 2008; Accepted: February 19, 2008; DOI: 10.1002/mats.200800004

Keywords: ABS; bulk process; grafting efficiency; modeling; synthesis

[1] H. Münstedt, *Polym. Eng. Sci.* **1981**, *21*, 259.
[2] H. Kubota, *J. Appl. Polym. Sci.* **1975**, *19*, 2299.
[3] F. Ramsteiner, G. E. McKee, W. Heckmann, W. Fischer, M. Fischer, *Acta Polym.* **1997**, *48*, 553.
[4] G. Cigna, P. Lomellini, M. Merlotti, *J. Appl. Polym. Sci.* **1989**, *37*, 1527.
[5] G. F. Giaconi, L. Castellani, C. Maestrini, T. Riccò, *Polymer* **1998**, *39*, 6315.
[6] L. Castellani, R. Frassine, A. Pavan, M. Rink, *Polymer* **1996**, *37*, 1329.
[7] Y. Han, R. Lach, W. Grellmann, *J. Appl. Polym. Sci.* **2001**, *79*, 9.
[8] K. Sardelis, H. J. Michels, F. R. S. Allen, *Polymer* **1987**, *28*, 244.
[9] Y. Okamoto, H. Miyagi, M. Kakugo, K. Takahashi, *Macromolecules* **1991**, *24*, 5639.
[10] E. T. C. Mui, V. B. Boateng, J. F. Fellers, J. L. White, *J. Appl. Polym. Sci.* **1982**, *27*, 1395.
[11] V. D. Yenalyev, N. A. Noskova, B. D. Kravchenko, *Polym. Prep. ACS* **1975**, 308.
[12] J. D. Moore, *Polymer* **1971**, *12*, 478.
[13] E. R. Wagner, L. M. Robeson, *Rubber Chem. Technol.* **1970**, *43*, 1129.
[14] C. B. Bucknall, I. Côte, I. K. Partridge, *J. Mater. Sci.* **1986**, *21*, 301.
[15] M. Demirors, R. Veraert, C. Hermans, *Polymer Prep. ACS* **1999**, *40*, 2,71.
[16] M. Fischer, G. P. Hellmann, *Macromolecules* **1996**, *29*, 2498.
[17] F. M. Peng, *J. Appl. Polym. Sci.* **1986**, *31*, 1827.
[18] G. Soto, E. Nava, M. Rosas, M. Fuenmayor, I. M. González, G. R. Meira, H. M. Oliva, *J. Appl. Polym. Sci.* **2004**, *92*, 1397.
[19] D. D. Kekhaiov, B. K. Mikhnev, *Int. Polym. Sci. Technol.* **1985**, *12*, 70.
[20] R. Díaz de León, G. Morales, P. Acuña, J. Olivo, L. Ramos de Valle, *Polym. Eng. Sci.* **2005**, *45*, 1288.
[21] R. Díaz de León, PhD Thesis, Centro de Investigación en Química Aplicada, México, 2003.
[22] D. A. Elizarrarás, G. Morales, R. Díaz de León, *Proceedings of the World Polymer Congress - MACRO 2006, 41st International Symposium on Macromolecules*, Brazil, 2006.
[23] D. A. Elizarrarás, PhD Thesis, Centro de Investigación en Química Aplicada, México, 2007.
[24] A. Brydon, A. Burnett, G. G. Cameron, *J. Polym. Sci., Polym. Chem. Ed.* **1973**, *11*, 3255.
[25] D. A. Estenoz, J. R. Vega, H. M. Oliva, G. R. Meira, *J. Liq. Chromatogr. Release Technol.* **2002**, *25*, 2781.
[26] N. J. Huang, D. C. Sundberg, *Polymer* **1994**, *35*, 5693.
[27] V. K. Gupta, G. S. Bhargava, K. K. Bhattacharyya, *J. Macromol. Sci. Chem.* **1981**, *A16*, 1107.
[28] G. Riess, C. Beslin, J. L. Locatelli, J. L. Refregier, in: *Polymer Alloys*, D. Klempner, K. C. Frisch, Eds., Plenum Publ. Corp., New York 1977.
[29] A. Gasperowicz, W. Łaskawski, *J. Polym. Sci., Polym. Chem. Ed.* **1976**, *14*, 2875.
[30] A. Brydon, G. M. Burnett, G. G. Cameron, *J. Polym Sci., Polym. Chem. Ed.* **1974**, *12*, 1011.
[31] P. Manaresi, V. Passalacqua, F. Pilati, *Polymer* **1975**, *16*, 520.
[32] F. M. Peng, *J. Appl. Polym. Sci.* **1990**, *40*, 1289.
[33] D. A. Estenoz, G. R. Meira, *J. Appl. Polym. Sci.* **1993**, *50*, 1081.
[34] D. A. Estenoz, E. Valdez, H. M. Oliva, G. R. Meira, *J. Appl. Polym. Sci.* **1996**, *59*, 861.
[35] D. A. Estenoz, G. R. Meira, N. Gómez, H. M. Oliva, *AIChE J.* **1998**, *44*, 427.
[36] N. Casis, D. A. Estenoz, L. M. Gugliotta, H. M. Oliva, G. R. Meira, *J. Appl. Polym. Sci.* **2006**, *99*, 3023.
[37] C. V. Luciani, PhD Thesis, Universidad Nacional del Litoral, Argentina, 2006.
[38] W. A. Ludwico, S. L. Rosen, *J. Appl. Polym. Sci.* **1975**, *19*, 757.
[39] C. V. Luciani, D. A. Estenoz, G. R. Meira, N. García, H. M. Oliva, *Macromol. Theor. Simul.* **2007**, *16*, 703.
[40] D. Bertin, F. Coutand, M. Duc, C. Galindo, D. Gigmès, S. Marque, P. Tordo, B. Vuillemin, *e-Polymer* **2004**, *10*, 1.
[41] N. Casis, C. V. Luciani, D. A. Estenoz, M. Martinelli, M. Strumia, G. R. Meira, *e-Polymer* **2007**, *85*, 1.
[42] J. L. Locatelli, G. Riess, *Angew. Makromol. Chem.* **1972**, *27*, 201.
[43] J. L. Locatelli, G. Riess, *Angew. Makromol. Chem.* **1973**, *28*, 161.
[44] J. L. Locatelli, G. Riess, *J. Polym. Sci. Polym. Chem. Ed.* **1973**, *11*, 3309.
[45] J. L. Locatelli, G. Riess, *Angew. Makromol. Chem.* **1973**, *32*, 117.
[46] J. L. Locatelli, G. Riess, *Angew. Makromol. Chem.* **1974**, *35*, 57.
[47] R. A. Hayes, *J. Polym. Sci. Polym. Chem. Ed.* **1981**, *19*, 993.
[48] R. A. Hayes, S. Futamura, *J. Polym. Sci. Polym. Chem. Ed.* **1981**, *19*, 985.
[49] G. Bouquet, W. C. Kentie, P. J. de Theije, F. van Damme, *Polym. Prepr.* **1996**, *37*, 536.

DOI: 10.1002/mats.200800004

[50] V. H. Schuster, M. Hoffmann, K. Dinges, *Angew. Makromol. Chem.* **1969**, *9*, 131.
[51] L. H. Garcia-Rubio, M. G. MacGregor, A. E. Hamielec, *Adv. Chem. Ser.* **1983**, *203*, 311.
[52] D. J. Stein, G. Fahrbach, H. Adler, *Adv. Chem. Ser.* **1975**, 148.
[53] L. H. Garcia-Rubio, M. G. Lord, J. F. MacGregor, A. E. Hamielec, *Polymer* **1985**, *26*, 2001.
[54] M. J. R. Cavalcanti, J. C. Pinto, *J. Appl. Polym. Sci.* **1997**, *65*, 1683.
[55] W. H. Hwang, K. Y. Yoo, H. K. Rhee, *J. Appl. Polym. Sci.* **1997**, *64*, 1015.
[56] A. Keramopoulos, C. Kiparissides, *Macromolecules* **2002**, *35*, 4155.
[57] C. C. Lin, W. Y. Chiu, C. T. Wang, *J. Appl. Polym. Sci.* **1979**, *23*, 1203.
[58] E. Mendizabal, S. Velazquez, V. Gonzalez, C. F. Jasso, *Polym. Eng. Sci.* **1995**, *35*, 2.
[59] I. González, G. R. Meira, H. M. Oliva, *J. Appl. Polym. Sci.* **1996**, *59*, 1015.
[60] D. W. van Krevelen, P. J. Hoftyzer, "*Properties of Polymers. Their estimation and correlation with chemical structure*", Elsevier Scientific Publishing, New York 1976.
[61] A. Echte, *Adv. Chem. Ser.* **1989**, 222.
[62] H. Suzuki, V. B. F. Mathot, *Macromolecules* **1989**, *22*, 1380.
[63] J. Brandrup, E. H. Immergut, *Polymer Handbook*, 2nd. Ed., John Wiley & Sons, New York 1975.
[64] R. C. Reid, J. M. Prausnitz, T. K. Sherwood, "*The Properties of Gases and Liquids*", 3rd Ed., McGraw Hill, New York 1977.
[65] E. C. Ihmels, J. Gmehling, *Ind. Eng. Chem. Res.* **2003**, *42*, 408.